

Q -switching stability limits of Kerr-lens mode lockingShota Kimura, Shuntaro Tani , and Yohei Kobayashi**The Institute for Solid State Physics, The University of Tokyo, 5-1-5 Kashiwanoha, Kashiwa, Chiba 277-8581, Japan*

(Received 9 June 2020; accepted 18 September 2020; published 9 October 2020)

Q -switching instability restricts pulse shortening in Kerr-lens mode-locked lasers (KLMLs). However, Q -switching suppression in KLMLs has not been discussed to date because of the difficulty of treating the Kerr-lens effect theoretically. We investigated parameter ranges for stable Kerr-lens mode locking (KLM) against Q switching theoretically and experimentally. We found the parameters and ranges required to suppress Q switching in hard- and soft-aperture KLMLs. In soft-aperture KLMLs, both intracavity power and spatial mode matching between a pump beam and a cavity mode were found to be critical. These findings were verified experimentally using an Yb:Y₂O₃ KLML. Our results provide cavity design criteria for stable KLMLs against Q switching.

DOI: [10.1103/PhysRevA.102.043505](https://doi.org/10.1103/PhysRevA.102.043505)**I. INTRODUCTION**

Passively mode-locked femtosecond lasers have been used in fields including materials science, metrology, and laser materials processing. Most of these applications require pulse train stability in both the short term and the long term. Q -switching instability is a fundamental phenomenon that destabilizes the energy of the pulse train, as illustrated in Figs. 1(a) and 1(b). Haus showed that this instability originated from a fluctuation of the population inversion that was caused by a nonlinear optical loss [1]. Although the theory was used successfully to derive the stability limit for mode locking in general, the detailed mechanisms of the nonlinear effects involved, such as saturable absorption, nonlinear polarization rotation, and the Kerr-lens effect, were not discussed.

Kärtner *et al.* and Hönninger *et al.* developed Q -switching theory for passively mode-locked lasers that use semiconductor saturable absorber mirrors (SESAMs) [2–5]. They derived simple and comprehensive criteria for suppression of Q -switching instability. These criteria have since been used to design state-of-the-art lasers including high-repetition-rate femtosecond lasers [6,7], sub-100-fs lasers [8,9], and high-power thin-disk lasers [8,10]. In the derivation of their criteria, the authors assumed a flat-topped beam profile. However, this assumption is only valid when the spatial beam effect is negligible; therefore, their theory does not include the Kerr-lens effect.

Kerr-lens mode-locked lasers (KLMLs) are passive mode-locked lasers that are based on the Kerr-lens effect. These lasers generate pulses with the shortest duration among mode-locked lasers because of the instantaneous nature of Kerr lensing [11]. Recent progress in the development of KLMLs has extended their parameter ranges toward higher repetition rates [12–14], shorter pulse durations [11,15,16], and higher pulse energies [17–19]. In this laser development stage, some KLMLs have tended to show Q -switching instability. How-

ever, to the best of our knowledge, there is no clear insight available about the parameter ranges required to stabilize Kerr-lens mode locking (KLM) against Q switching. This lack of knowledge is caused by the difficulty in considering the dynamic changes of a spatial beam profile affected by the Kerr-lens effect theoretically. Consequently, exploration of stable KLMLs to date has been reliant on experience alone.

In this paper, we derive simple criteria to suppress Q switching in KLMLs. The dynamic changes in Kerr lensing and their effects on a cavity mode were treated using a basic $ABCD$ matrix formalism. This paper considers two types of KLML: hard- and soft-aperture KLMLs. Our theoretical approach shows that the Q -switching instability restricts the pulse-shortening capability of the KLMLs. In addition, we found that this pulse-shortening limitation can be suppressed by increasing the intracavity power or improving the spatial mode matching between a pump beam and a cavity mode in the case of the soft-aperture KLMLs. These insights are summarized in a stability diagram with axes representing the averaged power and the pulse duration, as shown in Fig. 1(c). This diagram represents the possible pulse waveforms within a given cavity configuration. As a general perception, the peak power is the critical parameter required to start and sustain the KLM. This threshold peak power is drawn as a proportional relationship in the stability diagram. Our findings show that there is another threshold that limits the pulse shortening due to passive Q switching. Furthermore, we found that the stability region against Q switching could be extended by improving the spatial mode matching between the pump beam and the cavity mode. To verify our theoretical predictions, we performed experiments and plotted the resulting data in the stability diagram. Our theoretical results showed good agreement with our experimental results.

II. THEORY**A. Basic equations**

Q -switching instability in a passive mode-locked laser was first discussed by Haus [1]. This phenomenon was described

*yohei@issp.u-tokyo.ac.jp

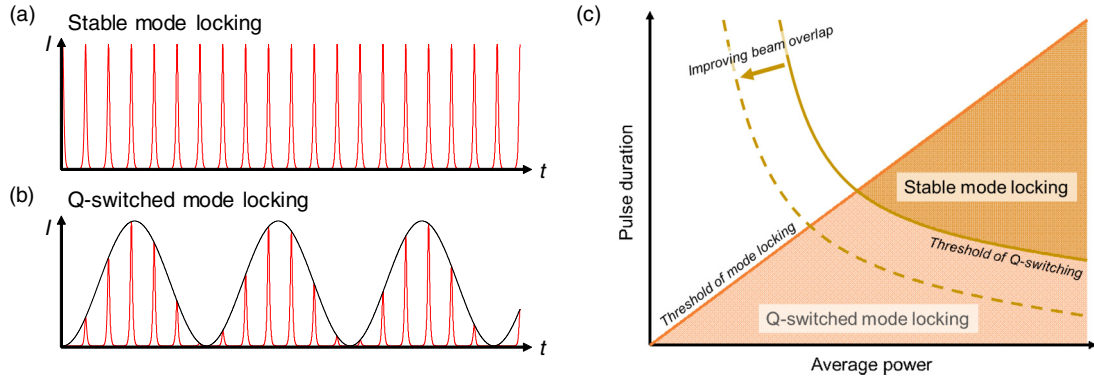


FIG. 1. Illustration of Q -switched mode locking. (a) Stable mode locking. (b) Q -switched mode locking. (c) Stability diagram of the Kerr-lens mode-locked laser for a given cavity configuration.

using the following two rate equations:

$$\frac{d}{dT}P = \frac{1}{T_R} [g - l - q(P)]P, \quad (1)$$

$$\frac{d}{dT}g = -\frac{1}{\tau_{\text{inv}}}(g - g_0) - \frac{P}{E_{\text{sat}}}g, \quad (2)$$

where T is the timescale of the pulse evolution during the cavity round trips, T_R is the round trip time, and P is the average power. Here g is the gain per round trip, l is the linear loss per round trip, q is the nonlinear loss per round trip, τ_{inv} is the upper state lifetime, g_0 is the small signal gain per round trip, and $E_{\text{sat}} = h\nu\pi w_g^2/2\sigma_{\text{em}}$ is the saturation energy of the gain. w_g is the beam radius of the cavity mode in the gain medium and σ_{em} is the emission cross section of the gain medium. Equation (1) is a simple master equation for the average power in a cavity. Equation (2) is a master equation for the gain that is based on a rate equation for the population difference in a four-level system. These equations are based on the following assumptions. First, it is assumed that the changes in the power, gain, loss, and nonlinear loss are all small ($<20\%$). Second, it is assumed that the changes in the temporal shapes of the pulse during a single cavity round trip are negligible; Eq. (1) thus does not include terms for the dispersion and self-phase modulation. These assumptions are all reasonable because the timescale for Q switching is long when compared with that of the cavity round trip time T_R .

Assume that these equations have steady-state solutions denoted by (\tilde{P}, \tilde{g}) . The stability of the steady-state solutions can be discussed using a linearized stability analysis, giving the following criterion against Q -switching instability [1–3]:

$$\frac{1}{\tau_{\text{inv}}} + \frac{\tilde{P}}{E_{\text{sat}}} > -\frac{\tilde{P}}{T_R} \left. \frac{dq}{dP} \right|_{\tilde{P}}, \quad (3)$$

where $1/\tau_{\text{inv}}$ is the decay rate of the population difference and \tilde{P}/E_{sat} is the stimulated transition probability. The left-hand side of Eq. (3) can be interpreted as the effective rate of gain recovery. The right-hand side represents the rate of change of the nonlinear loss. Therefore, the appearance of the Q switching is decided by the conflict between the gain recovery and the nonlinear loss. The mode locking remains stable when the gain recovery rate exceeds the rate of change of the nonlinear loss. In other words, the nonlinear loss must be suppressed

because it acts as positive feedback to any fluctuation. Note that this theoretical approach only clarifies whether or not the intracavity power remains stable against the Q -switching disturbance. The temporal profile of the Q -switched pulse train is not identified as part of this theory.

B. Overview for inclusion of the Kerr-lens effect

To derive a criterion for stable KLM, we rewrote the right-hand side of Eq. (3) to include the Kerr-lens effect and its spatial modulation explicitly. In the original equation given in Ref. [1], the derivative of the nonlinear loss is a function of the intracavity average power. However, the peak power is the most important physical quantity for Kerr lensing, which subsequently induces the change in the cavity loss. These processes are included explicitly as follows:

$$\left. \frac{dq}{dP} \right|_{\tilde{P}} = \frac{\tilde{P}_{\text{pk}}}{\tilde{P}} \left. \frac{dw}{dP_{\text{pk}}} \right|_{\tilde{P}_{\text{pk}}} \left. \frac{dq}{dw} \right|_{\tilde{w}}, \quad (4)$$

where w is the beam radius on the aperture, $P_{\text{pk}} = PT_R\beta/\tau$ is the peak power, τ is the pulse duration, and β is a numerical factor that is dependent on the pulse shape. The calculation of the two derivatives on the right-hand side is not straightforward because they are strongly dependent on the cavity design. In this paper, we made the following assumptions about the cavity design to simplify the discussion. First, an optical element that causes the nonlinear loss (aperture) is placed on the beam waist. In addition, this beam waist is located inside the Kerr medium, as shown in Fig. 2. These assumptions mean that the gain medium and the Kerr medium are the same in the case of the soft-aperture KLM. In this cavity configuration, Eq. (4) can then be rewritten as

$$\left. \frac{dq}{dP} \right|_{\tilde{P}} = \beta \frac{T_R}{\tau} \left. \frac{dw_0}{dP_{\text{pk}}} \right|_{\tilde{P}_{\text{pk}}} \left. \frac{dq}{dw_0} \right|_{\tilde{w}_0}, \quad (5)$$

where w_0 denotes the beam radius at the beam waist inside the Kerr medium. In the following sections, we consider the two derivatives shown in Eq. (5).

C. Beam mode change via the Kerr-lens effect

The spatial mode of the cavity with Kerr lensing was discussed by Haus *et al.* [20]. We modified their theory to

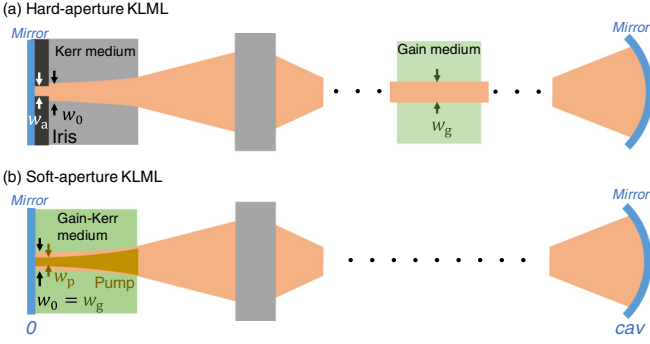


FIG. 2. Cavity geometry. We assumed that the Kerr medium is placed on one edge of the cavity. Our analysis fits the use of both plane and curved mirrors for the end mirror. (a) Hard-aperture KLML. (b) Soft-aperture KLML.

fit with our discussion (see the Appendix). Here, we express the peak-power dependence of the beam radius explicitly as $w(P_{pk})$. The beam radius at the beam waist that is modulated by the Kerr-lens effect can be expressed as

$$w_0(P_{pk}) = \sqrt{1 - \alpha \frac{P_{pk}}{P_{cr}}} w_0, \quad (6)$$

$$\alpha = \frac{2}{1 + (\frac{z_0}{L})^2} \left(1 - \frac{B^2 - z_0^2 A^2}{2LAB} \right), \quad (7)$$

where $P_{cr} = \lambda^2/4\pi n_0 n_2$ is the critical power of the Kerr effect, and n_0 and n_2 are the linear and nonlinear refractive indices of the Kerr medium, respectively. λ is the cavity mode wavelength, L is the length of the Kerr medium, $z_0 = \pi n_0 w_0^2(0)/\lambda$ is the Rayleigh length, and α is a cavity-design-dependent factor of the Kerr strength, where A , B , C , and D represent the matrix elements of a half-round trip of the linear cavity. In the case where the cavity is monolithic, $\alpha = 1$. In deriving these equations, we made the assumption that the peak power was small when compared with the critical power (i.e., $P_{pk}/P_{cr} < 10\%$).

From Eqs. (3), (5), and (6), we derived a basic criterion for the Q -switching instability in the KLML:

$$\frac{T_R}{\tau_{inv}} + \frac{\tilde{F}}{F_{sat}} > \alpha \frac{\tilde{P}_{pk}}{P_{cr}} \frac{\tilde{w}_0}{2} \left. \frac{dq}{dw_0} \right|_{\tilde{w}_0}, \quad (8)$$

where F is the pulse fluence inside the gain medium and $F_{sat} = h\nu/\sigma_{em}$ is the saturation fluence of the gain. Here, we have assumed that $\alpha P_{pk}/P_{cr} \ll 1$. The output power becomes stable against Q switching when the KLML satisfies the condition above, which means that strong decay of the population inversion when compared with the nonlinear loss is preferred to stabilize the mode locking. Note that the pulse duration only affects the peak power in Eq. (8) and that the shorter pulse duration is not preferred for stable KLM. This insight is reasonable because a strong nonlinear loss increases the fluctuation. As we discuss later, stable KLM with shorter pulse durations can be realized by minimizing dq/dw_0 . The derivative is dependent on the structure of the optical element that causes the nonlinear loss. We discuss two types of optical elements here: a hard aperture and a soft aperture.

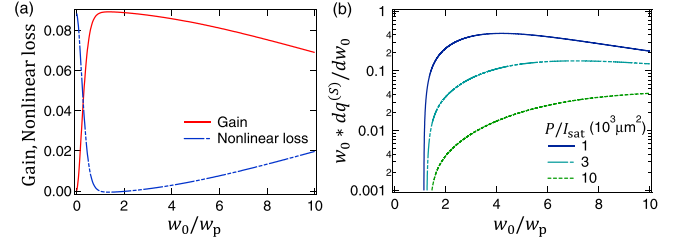


FIG. 3. Effective nonlinear loss characteristics of the soft aperture. (a) Calculated gain and effective nonlinear loss. $w_p = 6 \mu\text{m}$, $P_{abs} = 500 \text{ mW}$, $I_{sat} = 50 \text{ kW/cm}^2$, and $P/I_{sat} = 10^4 \mu\text{m}^2$. (b) Intra-cavity average power dependence of the derivative of the effective nonlinear loss.

D. Hard aperture

KLM using a hard aperture is an established method. This technique is based on the loss difference between continuous-wave lasing and the mode locking caused by a spatial aperture in a cavity. The nonlinear loss is induced by the mechanical iris, as illustrated in Fig. 2(a). The loss is then calculated as follows:

$$Pq^{(H)} = \frac{2P}{\pi w^2} \int_{w_a}^{\infty} e^{-2(\frac{r}{w})^2} 2\pi r dr = P e^{-2(\frac{w_a}{w})^2}, \quad (9)$$

where $q^{(H)}$ is the nonlinear loss induced by the hard aperture and w_a is the radius of the hard aperture. Here, we assume that the hard aperture is located on the beam waist, as mentioned earlier. Using Eqs. (8) and (9), we can then derive the Q -switching criterion for hard-aperture KLM as follows:

$$\frac{T_R}{\tau_{inv}} + \frac{\tilde{F}}{F_{sat}} > 2\alpha \frac{\tilde{P}_{pk}}{P_{cr}} \left(\frac{w_a}{\tilde{w}_0} \right)^2 e^{-2(\frac{w_a}{\tilde{w}_0})^2}. \quad (10)$$

Equation (10) indicates that a small beam radius when compared with the aperture radius can greatly extend the mode-locking stability range because of the exponential function on its right-hand side. In other words, the nonlinear loss from the hard aperture must be small to prevent Q switching. In contrast, a small nonlinear loss is disadvantageous for induction of mode locking [21,22]. In this sense, there is thus an appropriate nonlinear loss to both start the hard-aperture KLM and suppress the Q -switched KLM.

E. Soft aperture

A soft aperture is an effective aperture induced using the spatial gain profile, so we must therefore take the spatial beam profile into account in Eqs. (1) and (2). To simplify the discussion, we assume cylindrical Gaussian profiles for both the pump beam and the cavity mode inside the gain medium. We also assume an ideal four-level system, so the small signal gain can be written as $g_0(r) = \tau_{inv} \sigma_{inv} I_p \exp(-2r^2/w_p^2)/h\nu_p$, where ν_p is the wave number of the pump beam, w_p is the pump beam radius, $I_p = 2P_{abs}/\pi w_p^2$ is the absorbed pump intensity, and P_{abs} is the absorbed power [23]. Under these assumptions at the steady state, the gain can then be

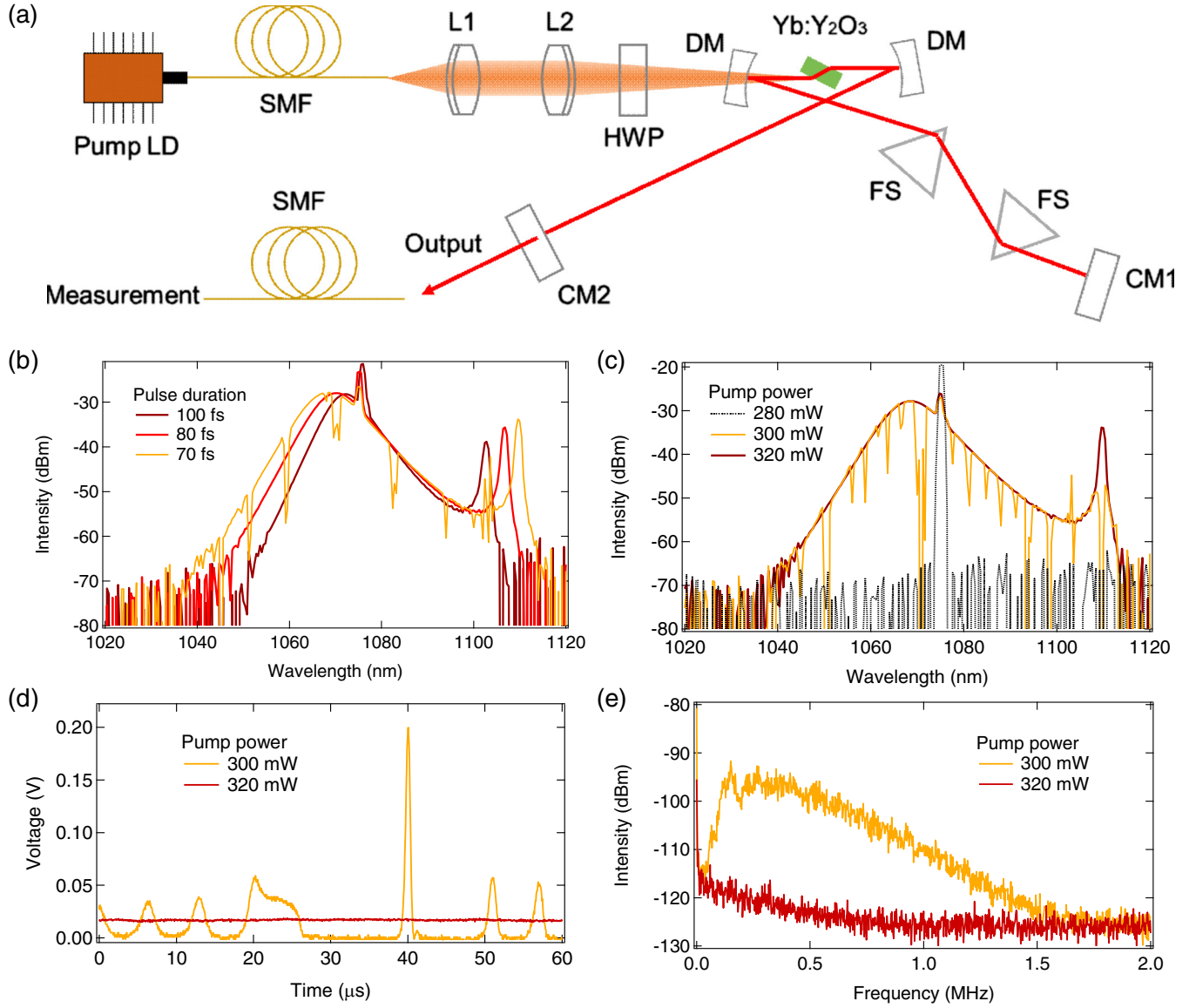


FIG. 4. (a) Experimental setup. LD, laser diode; SMF, single-mode fiber; HWP, half-wave plate; DM, dichroic mirror; FS, fused silica; CM, chirped mirror. (b) Optical spectra for various pulse durations. (c) Pump-power dependence of the optical spectrum. (d) Snapshots of the pulse train during both stable and Q -switched operations. (e) Radio-frequency spectra of both the stable and the Q -switched pulse trains.

written as

$$\begin{aligned}
 P g(w) &= \int_0^\infty \frac{g_0(r)}{1 + \frac{I(r)\tau_{\text{inv}}}{F_{\text{sat}}}} I(r) 2\pi r dr \\
 &= P \frac{h\nu}{h\nu_p} \frac{I_p}{I_{\text{sat}}} \int_0^1 \frac{u \frac{w_0^2}{w_p^2}}{1 + \frac{1}{I_{\text{sat}}} \frac{2P}{\pi w_0^2}} du,
 \end{aligned} \quad (11)$$

where ν is the wave number of the cavity mode and $I_{\text{sat}} = F_{\text{sat}}/\tau_{\text{inv}}$ is the saturation intensity. We substituted $u = \exp(-2r^2/w^2)$ for the integration variable to simplify the calculations.

Our discussion above is based on the nonlinear loss. Here, we rewrite the gain as

$$g(w) \equiv g_m - q^{(S)}(w), \quad (12)$$

where $g_m \equiv g(w_p)$ denotes the gain when the pump beam and the cavity mode are perfectly matched and $q^{(S)}(w)$ is the effective nonlinear loss, which is the amount of mismatch between the pump mode and the cavity mode. We assumed that the gain medium and the Kerr medium are the same, so the beam radius w_g in the gain medium is same as the beam radius w_0 in the Kerr medium. Under these conditions, the Q -switching stability limit can be derived as follows:

$$\frac{T_R}{\tau_{\text{inv}}} + \frac{\tilde{F}_0}{F_{\text{sat}}} > \alpha \frac{\tilde{P}_{\text{pk}}}{P_{\text{cr}}} \frac{\tilde{w}_0}{2} \left. \frac{dq^{(S)}}{dw_0} \right|_{\tilde{w}_0}, \quad (13)$$

$$\left. \frac{dq^{(S)}}{dw_0} \right|_{\tilde{w}_0} = - \frac{h\nu}{h\nu_p} \frac{I_p}{I_{\text{sat}}} \left. \frac{d}{dw_0} \int_0^1 \frac{u \frac{w_0^2}{w_p^2}}{1 + \frac{1}{I_{\text{sat}}} \frac{2P}{\pi w_0^2}} du \right|_{\tilde{w}_0}, \quad (14)$$

TABLE I. Experimental parameters.

Parameter	Value	Reference
w_p	6 μm	Measured
P_{abs}	250 mW	Measured at the intracavity power of 11 W
n_0	1.9	Ref. [25]
n_2	$2.52 \times 10^{-15} \text{cm}^2/\text{W}$	Ref. [25]
λ	1075 nm	Measured
λ_p	976 nm	Measured
σ_{em}	$0.3 \times 10^{-20} \text{cm}^2$	Ref. [26]
τ_{inv}	0.85 ms	Ref. [27]
β	0.88	Pulse shape of sech2
R	20 mm	Curvature of the concave mirrors
L	0.5 mm	Half length of the gain medium
l_1	100 mm	Length between concave mirror and end mirror
l_2	$l_2 \sim R/2 - L/n_0$	Length between concave mirror and gain medium
$\begin{pmatrix} A & B \\ C & D \end{pmatrix}$	$\begin{pmatrix} 1 & l_1 \\ 0 & 1 \end{pmatrix} \begin{pmatrix} 1 & 0 \\ -2/R & 1 \end{pmatrix} \begin{pmatrix} 1 & l_2 \\ 0 & n_0 \end{pmatrix} \begin{pmatrix} 1 & 0 \\ 0 & n_0 \end{pmatrix} \begin{pmatrix} 1 & L \\ 0 & 1 \end{pmatrix}$	Matrix elements

where F_0 is the fluence inside the gain-Kerr medium. In specific cases where one of the terms on the left-hand side of Eq. (13) is negligible, Eq. (13) can then be simplified to read

$$P_{\text{cr}} \tau > \alpha \beta \tau_{\text{inv}} \tilde{P} \frac{h\nu}{h\nu_p} \frac{I_p}{I_{\text{sat}}} \frac{\tilde{w}_0^2 \tilde{w}_p^2}{(\tilde{w}_0^2 + \tilde{w}_p^2)^2} \left(\frac{\tilde{I}_0}{F_{\text{sat}}} \ll \frac{1}{\tau_{\text{inv}}} \right), \quad (15)$$

$$P_{\text{cr}} \tau > \alpha \beta F_{\text{sat}} \frac{\pi \tilde{w}_0^2}{2} \frac{\tilde{w}_0}{2} \frac{dq^{(S)}}{dw_0} \Big|_{\tilde{w}_0} \left(\frac{\tilde{I}_0}{F_{\text{sat}}} \gg \frac{1}{\tau_{\text{inv}}} \right), \quad (16)$$

where $\tilde{I}_0 = 2\tilde{P}/\pi \tilde{w}_0^2$ is the intensity inside the gain-Kerr medium. Equation (15) is applicable where the population-difference decay rate is dominant when compared with the stimulated transition probability, while Eq. (16) is applicable under the opposite condition.

In general, well-established lasers tend to follow Eq. (16) because of its parameter ranges (i.e., the large $\sigma_{\text{em}} - \tau_{\text{inv}}$ product of the gain medium and the high intracavity average power). Because it is difficult to solve the integration given in Eq. (14) analytically, we calculated the gain and the effective nonlinear loss numerically, as shown in Fig. 3(a). The nonlinear loss curve has a minimum point near the perfect beam-matching condition. In this situation, the cavity satisfies the conditions of Eq. (16) easily, meaning that stable mode locking with shorter pulse durations is then possible. The spatial mode matching between the pump beam and the cavity mode can be improved by optimizing the cavity design and the alignment.

The integral in Eq. (14) includes the intracavity average power. This parameter also plays a significant role because it changes the function form of the effective nonlinear loss. Figure 3(b) shows the intracavity average power dependence of the derivative of the nonlinear loss. The data show that a high average power makes this derivative much smaller. This means that a high intracavity average power tends to stabilize mode locking against Q switching in the case of Eq. (16). Interestingly, the intracavity average power and the beam mode matching in Eq. (15) show the opposite trend to that in Eq. (16), so we must therefore select both the intracavity

power and the pump beam matching carefully, depending on the condition of the gain medium.

F. KLM with saturable absorbers

Some laser systems with saturable absorbers have demonstrated the Kerr-lens effect inside a laser crystal [24]. In this case, the Q -switching stability limit of the laser must include the effects of both the Kerr-lensing behavior and the saturable absorber. Here, we express the nonlinear loss from Eq. (1) as $q + q_A$, where q_A is the nonlinear loss caused by the saturable absorber. Assuming that SESAMs can be regarded as saturable absorbers, the Q -switching stability limit for SESAM-based mode-locked lasers can be derived as follows:

$$\frac{T_R}{\tau_{\text{inv}}} + \frac{\tilde{E}}{E_{\text{sat}}} > \alpha \frac{\tilde{P}_{\text{pk}}}{P_{\text{cr}}} \frac{\tilde{w}_0}{2} \frac{dq}{dw_0} \Big|_{\tilde{w}_0} + \Delta R \frac{E_{\text{sat,A}}}{\tilde{E}}, \quad (17)$$

where E is the pulse energy, ΔR is the maximum change in the nonlinear reflectivity, and $E_{\text{sat,A}}$ is the absorber saturation energy [3]. It is clear that one of the terms on the right-hand side is negligible in most laser systems. In the case where the Kerr-lens effect is negligible, Eq. (17) then corresponds to the Q -switching stability limit of SESAM-based mode-locked lasers given in Ref. [3].

III. EXPERIMENTS AND DISCUSSION

We constructed a soft-aperture KLML to verify our theory. The experimental setup is shown schematically in Fig. 4(a). To investigate the boundary of the Q -switching instability, we selected the 3 at. % Y_2O_3 ceramic as the gain medium; this medium shows a strong Kerr effect because of its high nonlinear refractive index (see Table I). The pump source was a wavelength-stabilized 976-nm laser diode that was coupled into a single-mode fiber, thus enabling high-beam-quality focusing. Two dichroic mirrors with identical curvatures of 20 mm were used and two flat mirrors with negative chirps (550 fs² and 650 fs²) were placed at the edge of the cavity. Both mirrors were placed at the same optical length from

the curved mirror to simplify the calculations. A prism pair was also inserted to vary the pulse duration without changing the other cavity parameters. After cavity optimization, KLM was achieved. The output beam was coupled to a single-mode fiber that was connected to the measurement instruments. The repetition rate of the pulse train was measured to be 600 MHz using a radio-frequency (RF) spectrum analyzer (FSV, 40 GHz, Rohde & Schwarz). Table I lists the parameters of our cavity. Within these parameter ranges, the stimulated transition probability is dominant when compared with the population-difference decay rate, meaning that Eq. (16) is appropriate for comparison with our results.

According to Eq. (8) or Eq. (16), KLM with shorter pulse durations causes the Q switching. We confirmed this prediction by varying the insertion length of the prism, which enables pulse duration tuning because the net cavity dispersion is varied. Figure 4(b) shows the output optical spectra obtained for various prism insertion lengths that were measured using an optical spectrum analyzer (AQ6373, Yokogawa). As the insertion length of the prism increased, the optical spectrum broadened in tandem, which indicates that the pulse duration in the cavity was shortened. When the pulse duration reached 70 fs, the mode locking became unstable, thus following the calculations using Eq. (16). Under this unstable condition, we varied the intracavity power by changing the pump power. Figure 4(c) shows the pump-power dependence of the optical spectrum. Increasing the pump power caused the mode locking to become stable. This behavior is also well matched with our calculation results, as shown in Fig. 3(b). The timing of the pulse train and its RF spectrum were measured to verify the time scale of the instability, with results as shown in Figs. 4(d) and 4(e). We observed envelope fluctuations due to Q switching with a timescale of a few hundred kHz. This timescale corresponds to the typical timescale for Q switching [5]. Note that each pulse train cannot be observed in Fig. 4(d) because we used an oscilloscope with a resolution bandwidth of 70 MHz, which lies below the pulse repetition frequency of 600 MHz.

It is clear that the experimental data show the same trends as our theory. We also compare the experimental data with the results from the theory quantitatively. Three parameters, i.e., the pulse duration, the intracavity power, and the spatial mode matching between the pump beam and the cavity mode, play significant roles in the laser stability when the cavity configuration has been determined. Using these important parameters, we drew a stability diagram for the soft-aperture KLML using Eq. (16), as shown in Fig. 5. Here, we assumed that $P_{\text{abs}} \propto P$. The experimental data mentioned above were also plotted in Fig. 5. As mentioned earlier, spatial mode matching between the pump beam and the cavity mode extends the parameter range for stable mode locking. Therefore, optimization of the cavity design and the alignment are among the most important factors in stabilization of mode locking. Note that it is difficult to determine the cavity mode diameter accurately from the cavity geometry alone because the KLM occurs near the edge of the cavity stability point. If the radius ratio between the pump beam and the cavity mode w_0/w_p is close to 1.5, our theory then explains the results well. These results prove that KLM with shorter pulse durations can be achieved by increasing the intracavity power or improving the

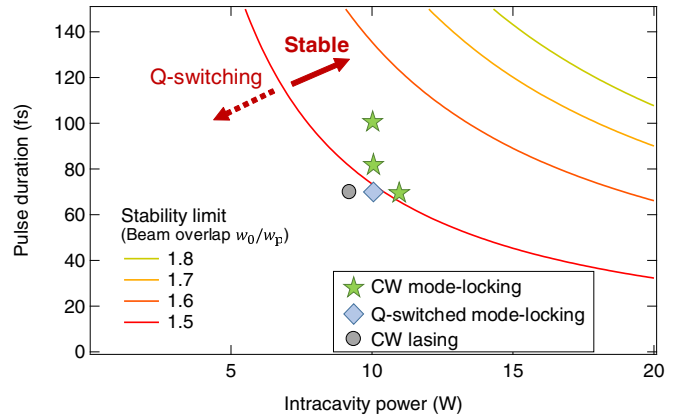


FIG. 5. Stability diagram. Each colored line indicates the Q -switching stability limit at a given w_0/w_p based on Eq. (16). The plot shows the measured values as shown in Figs. 4(b) and 4(c).

spatial mode matching between the pump beam and the cavity mode.

IV. CONCLUSIONS

In conclusion, we have investigated Q -switching instability in KLMLs. We derived simple criteria for both hard and soft apertures to suppress Q switching. The theory shows that Q switching restricts the pulse shortening of the mode-locked lasers. In a hard-aperture KLML, we found that the nonlinear loss must be low to suppress Q switching. In the well-established soft-aperture KLML, we found that high intracavity average power was preferred for stable mode locking. Furthermore, spatial mode matching between the pump beam and the cavity mode expands the parameter ranges for stable mode locking, which means that both the design and the alignment of the cavity are key factors for stabilization of the mode locking. Our research contributes to the design and control of various types of KLMLs, including high-repetition-rate, high-pulse-energy, and short-pulse-duration lasers.

ACKNOWLEDGMENTS

S.K. acknowledges support from a Japan Society for the Promotion of Science (JSPS) Grant-in-Aid (Grant No. 18J21520) and from the New Energy and Industrial Technology Development Organization (NEDO).

APPENDIX: CAVITY BEAM MODE WITH THE KERR-LENS EFFECT

The cavity spatial modes that are affected by Kerr lensing were discussed by Haus *et al.* [20]. We assume that the cavity geometry is as shown in Fig. 2. The complex beam parameter at the reference cross section (0) in Fig. 2 is $q_0 = jz_0$, where $z_0 = \pi n w_0^2 / \lambda$ is the Rayleigh range. In the absence of the Kerr effect, the q parameter at the reference cross section (cav) can be written as

$$q_{\text{cav}} = \frac{Aq_0 + B}{Cq_0 + D}, \quad (\text{A1})$$

where A , B , C , and D are the matrix elements of the half-round trip of the linear cavity.

The q parameter when passing through a Kerr medium with thickness L can be represented as [20]

$$q_L^K = q_0 + L + \delta q^K, \quad (\text{A2})$$

$$\delta q^K = -K \frac{2z_0 L}{z_0^2 + L^2} (z_0 - jL), \quad (\text{A3})$$

where $K = P/P_{\text{cr}}$ is the Kerr strength. By assuming the input q parameter to be $q_0^K = q_0 + \delta q^K$, we can then treat the Kerr effect using a standard $ABCD$ matrix analysis.

The beam curvature at the reference cross section (cav) should be equal to the curvature of the end mirror ($1/R$). Therefore, the following boundary condition should hold:

$$\frac{1}{R} = \text{Re} \left[\frac{1}{q_{\text{cav}} + \delta q_{\text{cav}}^K} \right] = \text{Re} \left[\frac{1}{q_{\text{cav}}} \right] - \text{Re} \left[\frac{1}{q_{\text{cav}}^2} \delta q_{\text{cav}}^K \right], \quad (\text{A4})$$

where δq_{cav}^K represents the change in the q parameter at the end mirror. Because $\text{Re}[1/q_{\text{cav}}] = 1/R$, the second term on the right-hand side of the equation must be zero. This condition can be described as

$$0 = \text{Re} \left[\frac{1}{q_{\text{cav}}^2} \frac{dq_{\text{cav}}}{dq_0} (\delta q^K + j\delta z_0) \right], \quad (\text{A5})$$

This means that the Kerr-induced change must be compensated by changing the cavity mode z_0 . Using Eqs. (A3) and (A5), we found that the Kerr-induced change in the cavity mode, δz_0 , can be described as

$$\frac{\delta z_0}{z_0} = -\alpha K, \quad (\text{A6})$$

$$\alpha = \frac{2}{1 + (\frac{z_0}{L})^2} \left(1 + \frac{z_0}{L} \frac{\text{Re} \left[\frac{1}{q_{\text{cav}}^2} \frac{dq_{\text{cav}}}{dq_0} \right]}{\text{Im} \left[\frac{1}{q_{\text{cav}}^2} \frac{dq_{\text{cav}}}{dq_0} \right]} \right), \quad (\text{A7})$$

Using Eq. (A1), Eq. (A7) can be written as Eq. (7) in Sec. II C. If the end mirror is a plane mirror, then Eq. (7) can be written using the relation $z_0^2 = -BD/AC$ as

$$\alpha = \frac{2}{1 + (\frac{z_0}{L})^2} \left(1 - \frac{AD + BC}{2LAC} \right), \quad (\text{A8})$$

The expressions in Eqs. (A6) and (A8) are very similar to the equations given in Ref. [20].

There are three differences between our formalism and that given in Ref. [20]. First, we considered the beam radius w_0 inside the Kerr medium rather than outside the Kerr medium. Second, δq_K represents a pure Kerr-lensing effect, whereas the insertion of a bulk Kerr medium was considered in Ref. [20]. Third, we considered the end mirror with an arbitrary radius of curvature, and not a plane mirror alone. These features are helpful in the development of our theory.

-
- [1] H. Haus, *IEEE J. Quantum Electron.* **12**, 169 (1976).
[2] F. X. Kaertner, L. R. Brovelli, D. Kopf, M. Kamp, I. G. Calasso, and U. Keller, *Opt. Eng.* **34**, 2024 (1995).
[3] C. Hönninger, R. Paschotta, F. Morier-Genoud, M. Moser, and U. Keller, *J. Opt. Soc. Am. B* **16**, 46 (1999).
[4] T. Schibli, E. Thoen, F. Kärtner, and E. Ippen, *Appl. Phys. B* **70**, S41 (2000).
[5] A. Schlatter, S. C. Zeller, R. Grange, R. Paschotta, and U. Keller, *J. Opt. Soc. Am. B* **21**, 1469 (2004).
[6] M. Mangold, C. A. Zaugg, S. M. Link, M. Golling, B. W. Tilma, and U. Keller, *Opt. Express* **22**, 6099 (2014).
[7] A. S. Mayer, C. R. Phillips, and U. Keller, *Nat. Commun.* **8**, 1 (2017).
[8] D. Waldburger, S. M. Link, M. Mangold, C. G. Alfieri, E. Gini, M. Golling, B. W. Tilma, and U. Keller, *Optica* **3**, 844 (2016).
[9] D. Okazaki, H. Arai, A. Anisimov, E. I. Kauppinen, S. Chiashi, S. Maruyama, N. Saito, and S. Ashihara, *Opt. Lett.* **44**, 1750 (2019).
[10] A. Diebold, T. Zengerle, C. Alfieri, C. Schriber, F. Emaury, M. Mangold, M. Hoffmann, C. J. Saraceno, M. Golling, D. Follman *et al.*, *Opt. Express* **24**, 10512 (2016).
[11] S. Rausch, T. Binhammer, A. Harth, J. Kim, R. Ell, F. X. Kärtner, and U. Morgner, *Opt. Express* **16**, 9739 (2008).
[12] A. Bartels, D. Heinecke, and S. A. Diddams, *Opt. Lett.* **33**, 1905 (2008).
[13] M. Endo, I. Ito, and Y. Kobayashi, *Opt. Express* **23**, 1276 (2015).
[14] S. Kimura, S. Tani, and Y. Kobayashi, *Optica* **6**, 532 (2019).
[15] P. Sévillano, P. Georges, F. Druon, D. Descamps, and E. Cormier, *Opt. Lett.* **39**, 6001 (2014).
[16] S. Kimura, S. Tani, and Y. Kobayashi, *Sci. Rep.* **9**, 1 (2019).
[17] J. Brons, V. Pervak, D. Bauer, D. Sutter, O. Pronin, and F. Krausz, *Opt. Lett.* **41**, 3567 (2016).
[18] N. Modsching, J. Drs, J. Fischer, C. Paradis, F. Labaye, M. Gaponenko, C. Kränkel, V. J. Wittwer, and T. Südmeyer, *Opt. Express* **27**, 16111 (2019).
[19] S. Kitajima, A. Shirakawa, H. Yagi, and T. Yanagitani, *Opt. Lett.* **43**, 5451 (2018).
[20] H. A. Haus, J. G. Fujimoto, and E. P. Ippen, *IEEE J. Quantum Electron.* **28**, 2086 (1992).
[21] T. Brabec, C. Spielmann, P. Curley, and F. Krausz, *Opt. Lett.* **17**, 1292 (1992).
[22] J. Herrmann, *J. Opt. Soc. Am. B* **11**, 498 (1994).
[23] A. E. Siegman, *Lasers* (University Science Books, Sausalito, CA, 1986).
[24] D. Sutter, L. Gallmann, N. Matuschek, F. Morier-Genoud, V. Scheuer, G. Angelow, T. Tschudi, G. Steinmeyer, and U. Keller, *Appl. Phys. B* **70**, S5 (2000).
[25] Y. Senatsky, A. Shirakawa, Y. Sato, J. Hagiwara, J. Lu, K. Ueda, H. Yagi, and T. Yanagitani, *Laser Phys. Lett.* **1**, 500 (2004).
[26] A. Shirakawa, K. Takaichi, H. Yagi, J. Bisson, J. Lu, M. Musha, K. Ueda, T. Yanagitani, T. Petrov, and A. Kaminskii, *Opt. Express* **11**, 2911 (2003).
[27] S. J. Beecher, T. L. Parsonage, J. I. Mackenzie, K. A. Sloyan, J. A. Grant-Jacob, and R. W. Eason, *Opt. Express* **22**, 22056 (2014).